LIMNOLOGY and OCEANOGRAPHY

ASLO

Limnol. Oceanogr. 65, 2020, 1200–1216

doi: 10.1002/lno.11384

Depth-dependent detritus production in the sponge, *Halisarca caerulea*

Michael P. Lesser,[1,2*] **Benjamin Mueller**,[3,4] **M. Sabrina Pankey**,[1] **Keir J. Macartney**,[1] **Marc Slattery**,[5] **Jasper M. de Goeij**[3,4]

[1]Department of Molecular, Cellular and Biomedical Sciences and, School of Marine Science and Ocean Engineering, University of New Hampshire, Durham, New Hampshire
[2]School of Marine Science and Ocean Engineering, University of New Hampshire, Durham, New Hampshire
[3]Department of Freshwater and Marine Ecology, Institute for Biodiversity and Ecosystem Dynamics, University of Amsterdam, Amsterdam, The Netherlands
[4]CARMABI Foundation, Willemstad, Curaçao
[5]Department of BioMolecular Science, University of Mississippi, Oxford, Mississippi

Abstract

Sponges are important ecological and functional components of coral reefs. Recently, a new hypothesis about the functional ecology of sponges in organic matter recycling pathways, the sponge-loop hypothesis, in which dissolved and particulate organic matter is taken up by sponges and shunted to higher trophic levels as detritus, has been proposed and demonstrated for shallow (< 30 m) cryptic species. However, support for this hypothesis at mesophotic depths (~ 30–150 m) is lacking. Here, we examined detritus production, a prerequisite of the sponge loop pathway, in a reciprocal transplant experiment, using *Halisarca caerulea* from water depths of 10 and 50 m. Detritus production was significantly lower in mesophotic sponges compared to shallow samples of *H. caerulea*. Additionally, detritus production rates in transplanted sponges moved in the direction of rates observed for resident conspecifics. The microbiome of these sponge populations was also significantly different between shallow and mesophotic depths, and the microbial communities of the transplanted sponges also shifted in the direction of their new depth in 10 d largely driven by changes in *Oxyphotobacteria*, *Acidimicrobiia*, *Nitrososphaeria*, *Nitrospira*, *Deltaproteobacteria*, and *Dadabacteriia*. This occurred in an environment where the availability of both dissolved and particulate trophic resources changed significantly across the shallow to mesophotic depth gradient where these sponge populations were found. These results suggest that changes in sponge detritus production are primarily driven by differential quality and quantity of trophic resources, as well as their utilization by the sponge host, and its microbiome, along the shallow to mesophotic depth gradient.

Sponges are an essential component of coral reef ecosystems (Wulff 2006; Pawlik 2011) that fill multiple ecological roles (Diaz and Rützler 2001; Bell 2008; Maldonado et al. 2012; de Goeij et al. 2017). An essential component of sponge ecology is that they host a diverse assemblage of symbiotic microorganisms (Hentschel et al. 2002, 2012; Taylor et al. 2007; Thacker and Freeman 2012) that facilitate the numerous functional roles of sponges including nutrient cycling, especially nitrogen, in coral reef ecosystems (Southwell et al. 2008; Fiore et al. 2010, 2013*a*,*b*; de Goeij et al. 2017). Sponges, through their autotrophic symbionts, also contribute to primary productivity (Thacker and Freeman 2012), and play a significant role in benthic-pelagic coupling via filtration of large quantities of dissolved (DOM) and particulate (POM) organic matter (Reiswig 1974; Pile 1997; Yahel et al. 2003; Lesser 2006; de Goeij et al. 2008*b*, 2017; Perea-Blázquez et al. 2012; Lesser and Slattery 2013, 2018). Additionally, the success of sponges on reefs is due, in part, to the numerous secondary metabolites that they and their symbiotic microbes produce and their cellular plasticity during wound repair (Alexander et al. 2015; Slattery et al. 2016) both of which play important roles in their defense against predators, competitors, and pathogens (Pawlik 2011). As coral reefs are affected by climate change stressors (e.g., ocean warming and acidification), it has been predicted that sponges will increase in abundance and be increasingly dominant functionally on coral reefs in the future (Bell et al. 2018*a*,*b*).

A recent hypothesis related to the trophic ecology of sponges on coral reefs has been proposed that has promoted a reevaluation of our understanding of the role of sponges on

*Correspondence: mpl@unh.edu

Additional Supporting Information may be found in the online version of this article.

coral reefs. Sponges consume large amounts of DOM, both dissolved organic carbon (DOC) and dissolved organic nitrogen (DON) (Yahel et al. 2003; de Goeij et al. 2008*a*, 2013; Mueller et al. 2014*a*; McMurray et al. 2016; Hoer et al. 2018), contributing between 56% and 97% of their daily organic carbon intake (see table 1 in de Goeij et al. 2017). Sponge consumption of large amounts of DOM can result in the release of cellular debris, primarily choanocytes, that fuel a "sponge loop" detrital pathway of significant importance to higher trophic levels on coral reefs (de Goeij et al., 2013, 2017; Rix et al. 2016, 2018). We now know that the release of DOC is light dependent (Mueller et al. 2014*b*), and that consumption of either particulate organic carbon (POC) and/or DOC can produce sponge detritus (Maldonado 2015). One of the uncertainties regarding the sponge-loop hypothesis had been whether the production of detritus occurs in open reef sponges rather than just cryptic species. McMurray et al. (2018) examined the production of detritus in nine species of open reef sponges, both high microbial abundance (HMA) and low microbial abundance (LMA) species, and found that while HMA sponges consumed primarily DOC and LMA sponges consumed primarily POC in the form of picoplankton, none of the species examined produced significant amounts of detritus. However, other studies have shown net detritus production in tropical open reef sponges (Reiswig 1971; Yahel et al. 2003), using a similar methodology. Net detritus production is also not confined to tropical sponges, both cryptic and open reef, but found in temperate (Alexander et al. 2014; Maldonado 2015) and cold-water ecosystems (see table 2 in de Goeij et al. 2017). Another unresolved question related to the sponge-loop hypothesis is whether sponges found at mesophotic depths on coral reefs ($\sim$ 30–150 m), where sponges are a dominant component of these communities (Lesser and Slattery 2018), participate in the sponge-loop pathway (de Goeij et al. 2017; Lesser et al. 2018).

Mesophotic coral ecosystems are deep-reef communities whose community structure and function change with increasing depth based on the availability of light and trophic resources (Lesser et al. 2018). In particular, benthic primary producers, such as corals and macroalgae decrease in abundance with increasing depth due to light limitation, while sponges increase in abundance, measured as either sponge density or percent cover, along a shallow (< 30 m) to mesophotic depth gradient in many coral reef ecosystems (Lesser and Slattery 2018). This shift in benthic community composition is likely to also affect the availability of DOM, since benthic primary producers are considered to be an important source of bioavailable DOM on coral reefs (Haas et al. 2011; Mueller et al. 2014*b*). Furthermore, decreasing light levels reduce DOM release by benthic primary producers (Mueller et al. 2014*b*, 2016), which supports observations that DOM concentrations decrease with increasing depth (Torréton et al. 1997; Slattery and Lesser 2015; Mueller et al. 2017; Lesser et al. 2019). In contrast, we also know that POC increases with increasing depth into the mesophotic zone (e.g., Lesser 2006). Given these opposing gradients in DOM and POM across a depth gradient, the relative importance of DOM in sponge nutrition may decrease with depth while POM importance will increase. In this regard, Slattery and Lesser (2015) showed a shift in the relative DOC:POC composition of the diet of *Agelas conifera* (= *A. tubulata*). Sponges on the shallow reef (23 m) consumed primarily DOC to meet their carbon demand (97.4% $\pm$ 0.4% [SE] DOC vs. 2.6% $\pm$ 0.6 [SE] POC), whereas sponges at the upper mesophotic depth of 46 m consumed DOC and POC in similar amounts (43.9% $\pm$ 8.0% [SE] DOC vs. 56.1% $\pm$ 4.6 [SE] POC). However, no measurements of detritus production were made on these sponges. Given the lower C : N ratio of POM compared with DOM, one hypothesis is that the balance between new sponge growth, which includes the production of choanocyte chambers, and cell turnover might be shifted in favor of new sponge growth at deeper depths, resulting in mesophotic sponges producing less detritus (Hadas et al. 2009; de Goeij et al. 2017). Simultaneously, knowing that the symbiotic microbes of these sponges play an important role in the consumption and processing of DOM within the holobiont, the composition as well as any functional differences in these microbial communities may shift with food availability along a gradient from shallow to mesophotic depths.

As the production of detritus is a prerequisite for the existence of sponge loop pathway as originally described, we compared the detritus production of the sponge *Halisarca caerulea* on shallow and mesophotic reefs. We assessed several factors that change across a depth gradient, that might affect detritus production, including food availability and composition, temperature, light, and changes in the symbiotic microbial communities. We further conducted a reciprocal transplant experiment to compare the detritus production of *H. caerulea* from shallow (10 m) and upper mesophotic (50 m) depths. Additionally, we quantified the availability of potential food sources (DOM and POM) along a depth gradient from 0 to 61 m, and the quality (C : N ratio) of those resources specifically at 10 and 50 m. Bulk stable isotope analysis of both sponge tissue and detritus was performed to elucidate the primary food sources for individual sponges. Lastly, the microbiomes of shallow and mesophotic sponges were compared to assess potential differences in their contribution to sponge nutrition.

Materials and methods

Site characterization

Field work was conducted in November 2017 at the Caribbean Research and Management of Biodiversity (CARMABI) marine field station, and sponge samples were collected from shallow ($\sim$ 10 m) and mesophotic ($\sim$ 50 m) depths near Buoy 1 (12°07′28.65″N, 68°58′23.23″W), a fringing reef on the leeward side of Curaçao. The study site is characterized by an

$\sim$ 100 m wide sandy reef terrace with patchy coral communities, gradually sloping toward a drop-off at 10–12 m depth (van Duyl 1985). The fore-reef slopes at an angle of $\sim$ 30–40° until a sand flat is reached at a depth of 50–60 m. Temperature (°C) and downwelling irradiance (E_d) of photosynthetically active radiation were taken every minute over several days using HOBO Pendant Temperature/Light data loggers at each site (n = 3 for each depth). Measurements of irradiance were in lumens m^{-2}, and only used to express the percentage difference in downwelling irradiance (E_d) between sites. Depth profiles of photosynthetically active radiation (PAR: 400–700 nm) irradiance (E_d) with depth were taken using a single channel PAR recorder (RBRsoloPAR; RBR) fitted with a calibrated LiCor cosine-corrected, planar, sensor (LI 192SA).

Detritus production by *H. caerulea*

H. caerulea is an encrusting LMA sponge found in both cryptic (i.e., reef interstices, reef depressions, and caves) and open reef environments and has previously been shown to be involved in the sponge-loop detrital pathway on shallow coral reefs (de Goeij et al. 2013). Individual *H. caerulea* were sampled for a transplant experiment from the shallow reef terrace (10–12 m depth; n = 7–9 replicates) and the mesophotic fore-reef slope (45–50 m depth; n = 7–9 replicates) at the Buoy 1 station. Sponges originating from the shallow reef terrace are hereafter referred to as "shallow," whereas those sampled at the mesophotic fore-reef slope are referred to as "deep." Each individual sponge was collected from the reef framework using a hammer and chisel and transported to the experimental location at 10 m. Subsequently, the attached coral rock substrate was cleared of epibionts and the sponge specimens were trimmed to an average size ($\pm$ SD) of 9.3 $\pm$ 3.5 cm^2 (de Goeij et al. 2008*b*). Six identical experimental platforms were constructed from PVC pipes; three were installed at 10 m depth, and three platforms were installed at 50 m depth (Fig. S1A,B). The platforms were placed $\sim$ 2 m apart from each other along the 10 and 50 m isobaths, respectively, and were designed to suspend sponges, facing downward, above a glass funnel (diameter: 7.5 cm) resting in a 15 mL collection tube (Fig. S1A). This positioning facilitated the collection of detritus while preventing the sponges from becoming smothered in sediment and/or self-produced detritus. The trimmed *H. caerulea* specimens were secured in harnesses made of cable ties and fishing line, and were hung above an individual funnel/collection tube (Fig. S1A). Sponges were suspended $\sim$ 0.5 cm above the funnels to maximize the probability of catching released detritus, while still allowing sufficient water exchange to ensure food supply for the sponges. Each platform held five experimental samples (= sponges) and two similar sized pieces of sun-dried coral rock serving as controls for the experimental sponge detrital production (Fig. S1B).

Following a reciprocal transplant design, sponge treatments were designated as deep to deep (DD) controls, shallow to deep (SD) transplants, deep to shallow (DS) transplants, and shallow to shallow (SS) controls. To simulate reduced light conditions experienced by *H. caerulea* growing in cavities and overhangs and/or at mesophotic depths, green PVC roofing sheets were installed on top of the three shallow platforms (Fig. S1A). Placement of the green roofing sheets reduced the light intensity by > 90% to irradiances more typically experienced in cavities and overhangs (Scheffers et al. 2010; Alexander et al. 2015). Transparent roofing sheets were installed at mesophotic depths to simulate any alterations in hydrodynamic conditions experienced by shallow experimental sponges, and to maintain irradiances previously observed at these mesophotic depths (Lesser et al. 2018). Sponges were left to acclimatize for 1 week above glass funnels to ensure full recovery from collection and trimming, transplantation, and adjustment to new conditions (Alexander et al. 2015). All work carried out on the shallow reef terrace was conducted using SCUBA, whereas closed circuit rebreather diving was used at mesophotic depths. Collections and experiments were performed under the research permit (#2012/48584) issued by the Curaçaoan Ministry of Health, Environment and Nature (GMN) to the CARMABI foundation.

On 13 November 2017, all platforms including glass funnels, coral rock controls, and experimental sponges that had been acclimatized after handling were cleaned thoroughly with soft brushes to minimize contamination with detritus accumulated over the previous week. New collection tubes were placed underneath the funnels, and sponges were left undisturbed for an initial collection period of 24 h. Divers collected the individual samples of experimental sponge/rock control carefully by tapping each funnel which promoted all detritus on the glass surface to fall into the funnel below. Subsequently, the experimental sponge/rock control was held with one hand away from the funnel and with the other hand the glass funnel was delicately tapped and turned in circles to transfer detritus adhering to the glass into the collection tube. Once all detritus from the funnel was in the collection tube, the funnel was slowly removed and the collection tube was sealed with a screw cap. After these collections were concluded, platforms were cleaned, and new tubes were placed as described above. Collection tubes with detritus were transported to the nearby CARMABI research station and processed within 3 h. This initial collection of detritus was found to be compromised by divers kicking sediment into the funnels. Subsequently, a second collection period of 48 h was initiated and detritus was collected for both experimental and control samples and processed as described above. Following the acclimatization period and the detrital sample collection periods, all sponge specimens were removed from the transplant platforms and placed into individual plastic collection bags for transport to CARMABI Research Station for processing. Rates of detritus production were based on a 48 h collection after the sponges had acclimatized.

In the laboratory, collection tubes were centrifuged (7 min, rcf = 3825 $\times$ g, 6000 rpm) until detritus formed a solid pellet at the bottom of the tubes. Overlying seawater was decanted and

the detrital pellet was transferred into a pre-weighed 1.5 mL microcentrifuge tube. Ultrapure water was added and the pellet was resuspended to desalinate the sample. Subsequently, sample tubes were centrifuged (7 min, rcf = 14,000 × *g*, 12,000 rpm) and overlying water was removed with a transfer pipette. Subsequently, samples tubes were covered with parafilm and freeze-dried for 24 h before weighing. Rates of detritus production were calculated based on surface area normalized total production, minus control samples, and then divided by the number of days the experiment was conducted. Sponge tissue samples were also collected for 16s rRNA metagenetic, and bulk stable isotope analyses. Each individual specimen was dipped in filtered (0.2 um) seawater to remove any particulate material from the tissue surface. Strips of tissue were then excised from the sponge using sterile scalpels, taking care to avoid coral rock or crustose coralline algae found below the sponge tissues. Pieces of tissue for 16s rRNA metagenetic analyses were collected and placed in a DNA preservation buffer (Seutin et al. 1991) and frozen at −20°C. Tissue samples for bulk stable isotope analysis were freeze-dried for 24 h. Samples were transferred on ice to the University of New Hampshire (UNH) for subsequent analyses (see below).

Differences in abiotic factors between 10 and 50 m were assessed using a two-tailed *t*-test, whereas analyses conducted throughout the entire depth range were analyzed using type II regression and ANOVA. All experimental results were assessed for treatment effects using ANOVA after checking for normality and heteroscedasticity. Any values not meeting these requirements were transformed before analysis. Ratios are a priori not normally distributed and were transformed prior to analysis. Any significant treatment effects were then followed by post hoc pairwise Tukey's HSD to detect treatment effects.

Environmental analyses

Seawater samples (1 L) from the surface, 10, 15, 30, 46, 50, and 61 m (n = 3 per depth) were collected from the site and returned to the laboratory where they were each immediately filtered onto GF/F filters. Each GF/F filter was placed in a 2 mL cryovial with DNA preservation buffer (Seutin et al. 1991) and stored at −20°C for subsequent DNA extraction. The seawater filtrate was frozen, transported to UNH, and analyzed for dissolved inorganic nitrogen (DIN) consisting of nitrate/nitrite (NO_x: μmol L^{-1}) and ammonium (NH_4: μmol L^{-1}) using high throughput colorimetric assays on a Smartchem Chemistry Analyzer. The relative differences in laboratory duplicates averaged 4.6% for NO_x and 7.1% for NH_4, with average Certified Reference Material (CRM) recoveries of 102.6% for NO_x and 95% for NH_4. These same samples were analyzed for DOC (μmol C L^{-1}) and DON (μmol N L^{-1}) as total dissolved nitrogen (TDN) minus DIN, using high-temperature catalytic oxidation and high-temperature oxidation with chemiluminescent detection, respectively, at the UNH Water Quality Analysis Laboratory. The relative differences in laboratory duplicates averaged 4.9% for DOC and 7.8% for TDN, with average CRM recoveries of 97% for DOC and 102.1% for TDN.

For live POC, we analyzed aliquots (3 mL) of seawater from samples (100–200 mL) collected at the surface, 10, 15, 30, 46, and 61 m (n = 3 per depth). Acid washed and deionized water-rinsed 100 mL syringes were filled by divers ∼ 1–2 m from the benthos, regardless of substrate angle. These samples were returned to the laboratory and fixed at a final concentration of 0.5% electron microscopy grade paraformaldehyde in filtered (0.2 μm) seawater, and frozen at −80°C. Samples were shipped frozen and then maintained in liquid nitrogen until analysis by flow cytometry (Lesser et al. 1992; Lesser 2006). Each sample was analyzed for cell abundances using a Becton Dickinson FACScan flow cytometer equipped with a 15 mW, 488 nm, air-cooled Argon ion laser. Simultaneous measurements of forward light scatter (FSC, relative size), 90° light scatter (SSC), chlorophyll fluorescence (> 650 nm), and phycoerythrin fluorescence (560–590 nm) were made on all samples as described previously (Lesser et al. 1992; Lesser, 2006). Differentiation of cyanobacteria from prochlorophytes was based on the presence of phycoerythrin fluorescence. The volume of sample analyzed by the FACScan was determined gravimetrically, where the difference in mg was proportional to the volume of sample analyzed in mL. The abundance of heterotrophic bacteria was determined using SYBRGreen (Molecular Probes), a dsDNA specific dye, which stains all prokaryotes and picoeukaryotes (emission fluorescence: 515–525 nm). Subtraction of photosynthethic prokaryotes from the total prokaryotes provided the concentration of the heterotrophic bacterial component of the community, including numerous Archaea. Gating populations, based on size, allowed for the separation and enumeration of the picoeukaryotic fraction. All flow cytometry measurements included the analysis of fluorescent-calibrated beads of varying sizes to calculate the equivalent spherical diameter (ESD), and biovolume for cell populations, as needed. All enumerated cells were converted to carbon and nitrogen equivalents using the following conversions; *Synechococcus*: 470 fg C $cell^{-1}$ (Campbell et al. 1994), *Prochlorococcus*: 53 fg C $cell^{-1}$ (Morel et al. 1993), and heterotrophic bacteria: 20 fg C $cell^{-1}$ (Ducklow et al. 1993); and *Synechococcus*: 35 fg N $cell^{-1}$ (Bertilsson et al. 2003), *Prochlorococcus*: 9.4 fg N $cell^{-1}$ (Bertilsson et al. 2003), and heterotrophic bacteria: 3.3 fg N $cell^{-1}$ (FaggerBakke et al. 1996). For eukaryotic phytoplankton, the carbon and nitrogen contents were not calculated as the volume measurements required for C and N conversions were not available. However, the number of eukaryotic phytoplankton available in the plankton, and often consumed by sponges, was low (Lesser 2006).

Stable isotope analyses

Samples from each control and for all experimental sponges, and the detritus they produced (as described above), were sent to the Stable Isotope Laboratory at the Marine Biological Laboratory, and acidified using 1 N HCL to remove any inorganic carbon (sensu Jaschinski et al. 2008) for the bulk

analysis of particulate C and N, as well as the ratio of the natural abundance of the stable isotopes δ^{15}N and δ^{13}C. Samples were analyzed using a Europa ANCA-SL elemental analyzer-gas chromatograph attached to a continuous-flow Europa 20-20 gas source stable isotope ratio mass spectrometer. The carbon isotope results were reported relative to Vienna Pee Dee Belemnite, and nitrogen isotope results were reported relative to atmospheric air; both were expressed using the delta (δ) notation in units per mil (‰). The analytical precision of the instrument was $\pm$ 0.1‰, and the mean precision of sample replicates for δ^{13}C was $\pm$ 0.4 ‰, and for δ^{15}N was $\pm$ 0.2 ‰. The δ^{13}C and δ^{15}N tissue data were also used in a mixing model using the R package SIAR as described by van Duyl et al. (2018) to determine the proportional contribution of algal vs. coral DOM, as well as POM and detritus for sponges in each treatment. We used data from different sites in the Caribbean that are consistent with the known variation in these values. These inputs into the model included δ^{13}C and δ^{15}N values for algal DOM (δ^{13}C −15.42 ‰; δ^{15}N 0.80, average of *Dictyota* sp. and *Lobophora* sp., table 3 in van Duyl et al. 2018), and based on the assumption that autotrophic algal DOM is a reflection of isotopic value of its source), coral DOM (δ^{13}C −17.19‰; δ^{15}N 0.26, average of all coral species table 2 in van Duyl et al. 2011), and based on the assumption that autotrophic coral DOM is a reflection of the isotopic value of its source, POM (δ^{13}C −24.91 ‰; δ^{15}N 5.62, van Duyl et al. 2018) and detritus (δ^{13}C −19.54‰; δ^{15}N 2.56, from 10 and 50 m controls [no sponges]). A trophic enrichment factor of 0.5 $\pm$ 0.5% (SD) for δ^{13}C and 3.0 $\pm$ 0.5% (SD) for δ^{15}N was used (van Duyl et al. 2018).

DNA extraction and metagenetics

DNA was extracted from GF/F-filtered seawater and the preserved tissue and detrital pellets using the DNEasy PowerSoil DNA isolation kit (Qiagen), using manufacturer's instructions with modifications to cell lysis as described by Sunagawa et al. (2010), followed by two rounds of 2 min bead beating using a Qiagen QuickLyser set at 50 MHz. All microbial gDNA was checked for quality and concentration using a NanoDrop spectrophotometer 2000c.

Microbial samples were amplified using the polymerase chain reaction (PCR) with primer sets targeting the universal bacterial/archaeal 16S rRNA gene. Samples were amplified with new degenerate primers targeting the hypervariable region V3–V4, consisting of the forward primer 515F (5′-GTGYCAGCMGCCGCG GTAA; Parada et al. 2016) and the reverse primer 806R (5′-GGACTACNVGGGTWTCTAAT; Apprill et al. 2015). Fluidigm linker sequences CS1 (5′-ACACTGACGACATGGTTCTACA) and CS2 (5′-TACGGTAGCAGAGACTTGGTCT) were added to the 5′ end of both forward and reverse primers to facilitate Illumina MiniSeq. The 16S rRNA gene PCR consisted of a 25 μL reaction with 12.5 μL AmpliTaq Gold 360 Master Mix (Applied Biosystems), 1.0 μL GC-enhancer, 0.5 μL 515F (10 μmol L^{-1}) and 0.5 μL 806R (10 μmol L^{-1}), 2.0 μL of DNA template (40–60 ng), and 8.5 μL nuclease free water (Integrated DNA Technologies). Reactions were performed using the following protocol: initial denaturation for 10 min at 95°C, 30 cycles of 95°C for 45 s, 50°C for 60 s, and 72°C for 90 s, followed by a 10 min extension at 72°C. The PCR products were then electrophoresed on a 1% agarose gel.

Sequencing and bioinformatics

The 16S PCR amplicons containing Fluidigm linkers were sequenced on an Illumina MiniSeq System using the Mid-Output reagent kit (2 × 150 bp reads, ~ 20–40,000 reads per sample) at the University of Illinois at Chicago Research Resources Center's Sequencing Core. Amplicon sequence variants (ASVs) were inferred and tabulated across samples using DADA2 (Callahan et al. 2016). Briefly, raw reads were trimmed of the initial 20 bp to remove residual primer and then truncated beyond the first instance of quality scores below 3 (truncQ = 2). The maximum expected error during denoising was 2 (maxEE = 2). The error model was built from the first 100 M bases and inspected using "plotErrors." Denoised reads were then merged and chimeric contigs discarded using mergePairs. Taxonomic ranks were assigned to the inferred ASVs using the SILVA ribosomal reference database release 128, using the DADA2 function "assignTaxonomy."

Analyses of the sponge, detrital, and seawater microbial communities were accomplished using PhyloSeq functions in R (McMurdie and Holmes 2013). The ASV count table was first filtered to discard samples with fewer than 10,000 counts, and then filtered to include ASVs detected in more than 2 samples, and accounting for at least 10 occurrences across samples. Samples were then rarefied to normalize for sequencing effort. Alpha diversities were estimated using Shannon and Chao1 richness indices. Samples were ordinated based on Bray-Curtis distance using nonmetric multidimensional scaling (method = NMDS). In order to assess compositional differences at various taxonomic scales (kingdom, phyla, class, ASV, etc.), the rarefied ASV count table was consolidated by rank using the "tax_glom" function. Raw counts were transformed to center log ratios using the "transform" function (transform = CLR) from the R "microbiome" package (Lahti et al. 2017). Compositional differences among transplant treatments were then tested using PERMANOVA on sample Aitchison distances (Gloor et al. 2017) with the "adonis" function from the R package "vegan" (Oksanen et al. 2019). Tests for the effect of treatment in the abundances of dominant taxa (i.e., comprising > 1% of reads) used ANOVA and Tukey's HSD for post hoc treatment comparisons.

Metagenomic functional abundances were predicted from 16S abundances using *PICRUSt2* v2.1.0-b (https://github.com/picrust/picrust2/wiki). Briefly, 16S ASVs inferred by DADA2 were aligned with *HMMER* (Eddy 2008) and placed in the provided reference tree using *EPA-ng* and *GAPPA* (Barbera et al. 2019). Gene family copy numbers were predicted for 16S as well as KEGG functions (i.e., EC and KO accessions) using Hidden State Prediction (*castor*; Louca and Doebeli 2018) based on

16S ASV abundances and phylogenetic proximity to reference taxa with available genomes. Abundances of biological pathways encoded by microbiomes were then predicted using *MinPath* (Ye and Doak 2009). Abundances of KEGG accessions corresponding to metabolic processes of interest were tested for treatment effects using ANOVA (Table S2).

Results

Environmental variability along the shallow to mesophotic depth gradient

Environmental differences, where they existed, between experimental sites were assumed to reflect their depth specific variability. At 10 m, the average temperature during the deployment was 28.6°C ± 0.9°C (mean ± SD) and at 50 m it was 28.1°C ± 0.9°C, which was not significantly different between depths (two-tailed *t*-test, $t(14538) = 0.412$, $p = 0.680$). From the profile data ambient E_d at 10 m was ~ 740 μmol quanta m^{-2} s^{-1}, and at 50 m it was ~ 72 μmol quanta m^{-2} s^{-1}. The complete profiles of irradiance with depth can be seen in Lesser et al. (2018). Using a 90% and 10% decrease due to the green and transparent roofing sheets, the sponges were exposed to ~ 74 μmol quanta m^{-2} s^{-1} at 10 m, and ~ 65 μmol quanta m^{-2} s^{-1} at 50 m water depth. However, sponges at both depths were hanging upside down and receiving primarily upwelling irradiances (E_u) reflected off the sandy bottom. Given that the reflectance of these substrates can be affected by sediment type, presence of microphytobenthic organisms, and organic content, the reflectance of E_d can be anywhere from 30% to 55% across the visible spectrum (Louchard et al. 2003). Thus, we applied a 40% reduction in E_d to obtain values of E_u, or upwelling irradiance, as an estimate of what the experimental sponges were seeing during the acclimatization and experimental periods. This resulted in estimated E_u irradiances of ~ 44 μmol quanta m^{-2} s^{-1} at 10 m and 39 μmol quanta m^{-2} s^{-1} at 50 m. The combined nitrate and nitrite (NO_x) for 10 m was 1.35 μmol L^{-1} ± 0.03 (mean ± SD), and at 50 m it was 1.48 μmol L^{-1} ± 0.09. (mean ± SD). These changes were not significantly different between depths (two-tailed *t*-test, $t(4) = 2.56$, $p = 0.063$).

The trophic resources available to sponges varied significantly with increasing depth at the beginning of the experiment. For the dissolved fractions; both DOC (ANOVA: $F_{1,4} = 15.15$, $p = 0.03$) and DON (ANOVA: $F_{1,4} = 14.2$, $p = 0.033$) decreased significantly with increasing depth (Fig. 1A,B). At the end of the experiment, additional measurements of DOC and DON from the experimental sites revealed that DOC concentration at 10 m was 77.44 μmol C L^{-1} ± 1.85 (mean ± SD), and at 50 m it was 68.58 μmol C L^{-1} ± 0.65 (mean ± SD), which was significantly different between depths (two-tailed *t*-test, $t(4) = 7.83$, $p = 0.001$). The DON concentration at 10 m was 5.38 μmol N L^{-1} ± 0.55 (mean ± SD) and at 50 m it was 3.24 μmol N L^{-1} ± 0.99, (mean ± SD) which was also significantly different between depths (two-tailed *t*-test, $t(4) = 3.27$, $p = 0.031$). The C : N ratios for DOC: DON averaged 14.39 ± 0.65 (SE) at 10 m and 21.17 ± 4.05 at 50 m depth and were not significantly different from each other (two-tailed *t*-test, $t(4) = 1.97$, $p = 0.119$).

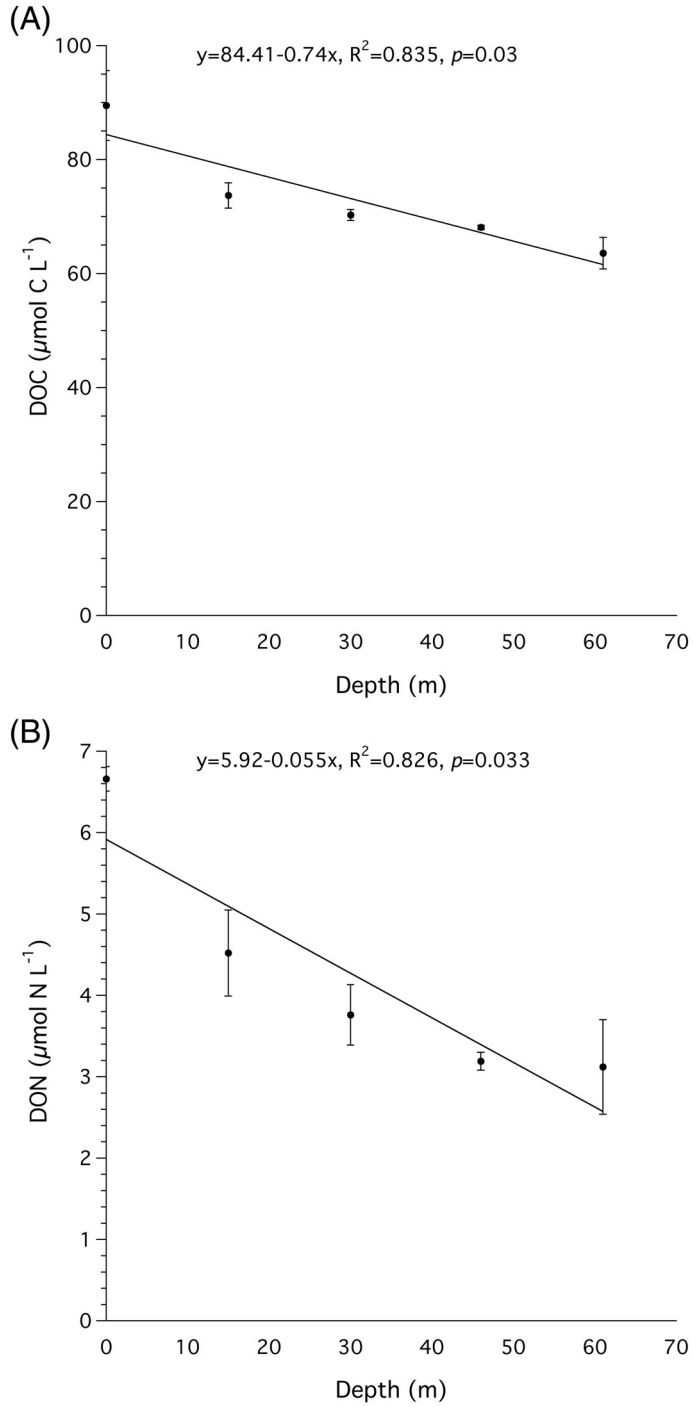

Fig. 1. (**A**) Water column DOC (mean ± SD) as a function of depth ($n = 3$ samples per depth) in Curaçao. A significant regression (ANOVA: $F_{1,4} = 15.15$, $p = 0.03$) was observed for DOC as a function of depth; (**B**) water column DON (mean ± SD) as a function of depth ($n = 3$ samples per depth) in Curaçao. A significant regression (ANOVA: $F_{1,4} = 14.2$, $p = 0.033$) was observed for DON as a function of depth.

As was the case for the dissolved fractions, the particulate fractions varied with depth. *Synechococcus* populations were a component of the picoplankton and declined significantly (ANOVA: $F_{1,5}$ = 22.82, p = 0.009) with increasing depth (Fig. 2A). In contrast prochlorophytes, another component of the picoplankton, increased significantly (ANOVA: $F_{1,5}$ =

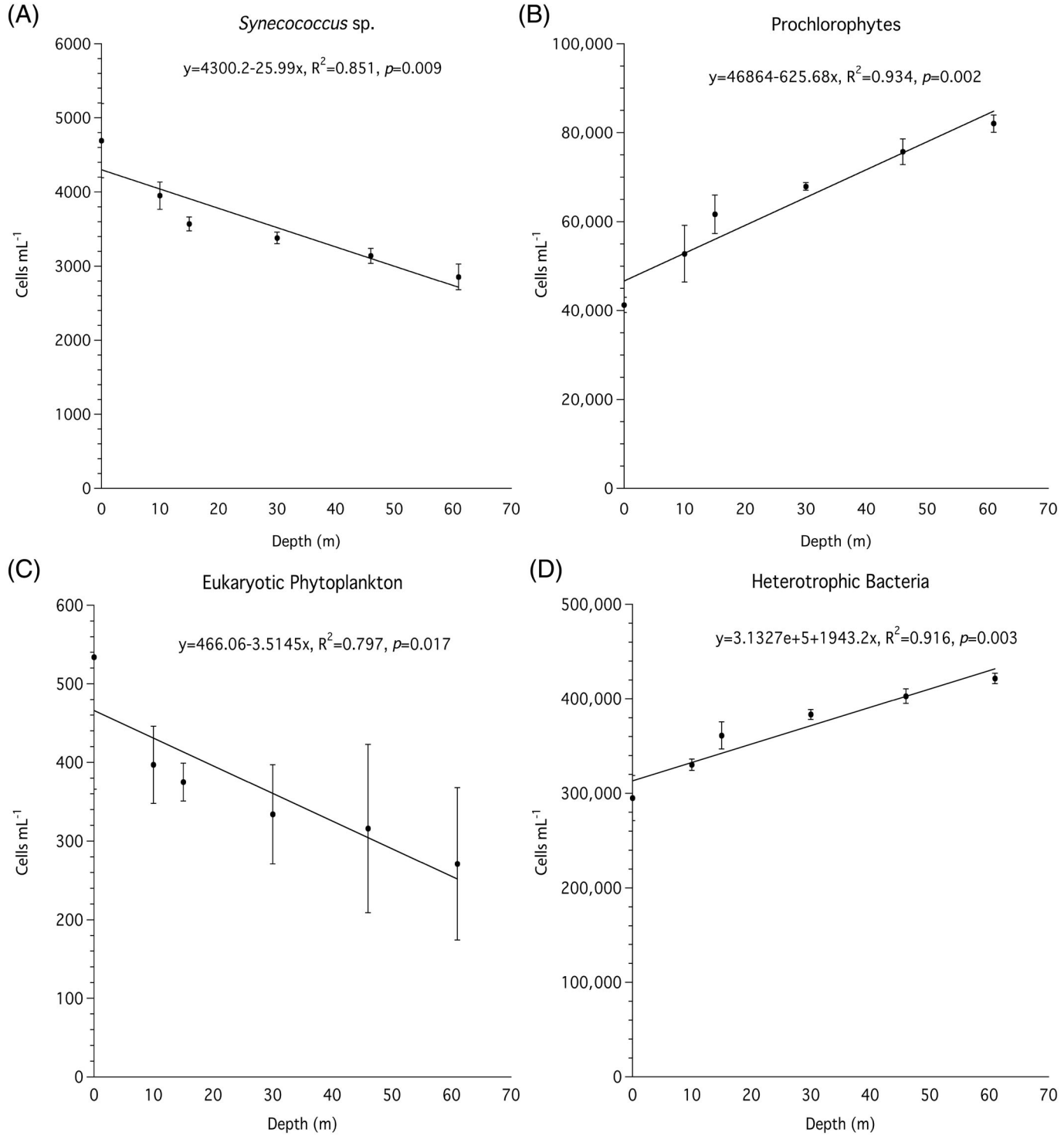

Fig. 2. Significant depth-dependent regressions for (**A**) *Synechococcus* (ANOVA: $F_{1,5}$ = 22.82, p = 0.009); (**B**) prochlorophytes (ANOVA: $F_{1,5}$ = 56.32, p = 0.002); (**C**) eukarytotic phytoplankton (ANOVA: $F_{1,5}$ = 17.71, p = 0.017); and (**D**) heterotrophic bacteria (ANOVA: $F_{1,5}$ = 43.46, p = 0.003) in Curaçao as a function of depth.

56.32, $p = 0.002$) with depth (Fig. 2B). Eukaryotic phytoplankton, found in the lowest total number at all depths, decreased significantly (ANOVA: $F_{1,5} = 17.71$, $p = 0.017$) with depth (Fig. 2C), while the largest component of the picoplankton, heterotrophic bacteria, increased significantly (ANOVA: $F_{1,5} = 43.46$, $p = 0.003$) with depth (Fig. 2D). When these components were converted to carbon and nitrogen equivalents, as described above, both POC (ANOVA: $F_{1,5} = 64.89$, $p = 0.0013$) and PON (ANOVA: $F_{1,5} = 49.05$, $p = 0.002$) increase significantly with depth (Fig. 3A,B). The C : N ratios averaged 5.16 ± 0.0003 (SE) at 10 m, and 5.01 ± 0.498 at 50 m depth, and were not significantly different from each other (two-tailed *t*-test, $t(4) = 308$, $p = 0.773$).

Detritus production by *H. caerulea*

The treatment effects on the corrected (i.e., sponge detritus minus control detritus) rates of detritus production for *H. caerulea* were significant (ANOVA: $F_{3,20} = 6.54$, $p = 0.0029$). Post hoc analysis revealed that SS produced significantly more detritus (1.358 ± 0.326 [SE] mg cm^{-2}) than DD sponges (0.284 ± 0.075 [SE] mg cm^{-2}) (Tukey's HSD, $p < 0.05$; Fig. 4) while the SD sponges (0.436 ± 0.102 [SE] mg cm^{-2}) were not significantly different from DD samples (Tukey's HSD, $p > 0.05$) and DS sponges (0.839 ± 0.137 [SE] mg cm^{-2}) showed intermediate rates of detritus production that were not significantly different from either SS or DD samples (Tukey's HSD, $p > 0.05$; Fig. 4).

Stable isotope signatures of *H. caerulea* tissues and detritus

At the end of the 10 d, experiment treatment effects for the δ^{13}C stable isotope values of *H. caerulea* tissue (Fig. 5) were not significantly different (ANOVA: $F_{3,28} = 0.817$, $p = 0.495$) whereas the δ^{15}N of the same tissues (Fig. 5) were significantly different (ANOVA: $F_{3,28} = 4.059$, $p = 0.016$). The post hoc Tukey's HSD analysis showed that for the tissue, δ^{15}N SS and DS were significantly lower compared to SD, with DD treatments indistinguishable from all other treatments (Tukey's HSD, $p < 0.05$). There was no effect of treatment (ANOVA: $F_{3,28} = 0.991$, $p = 0.412$) on tissue C : N ratios, which varied from 5.2 to 6.2. For the sponge-produced detritus samples, treatment effects for the δ^{13}C stable isotope values (Fig. 5) were significantly different (ANOVA: $F_{3,24} = 38.06$, $p < 0.0001$) with SS and DS treatments significantly enriched in ^{13}C compared to DD and SD treatments (Tukey's HSD, $p > 0.05$), while the δ^{15}N values of sponge detritus (Fig. 5) were not significantly different from each other (ANOVA: $F_{3,24} = 1.854$, $p = 0.164$). There was no effect of treatment (ANOVA: $F_{3,24} = 0.726$, $p = 0.546$) on C : N ratios which ranged from 7.9 to 9.2. The SIAR mixing model, which calculates the percentage of the sponge diet in each treatment that comes from different trophic sources in the water column, showed a significant effect of treatment for the percentage contribution of algal DOM (ANOVA: $F_{3,28} = 7.478$, $p = 0.0008$) with the only significant (Tukey's HSD, $p < 0.05$) pairwise comparison being the SD treatment compared to all other treatments, which were not significantly different (Tukey's HSD, $p > 0.05$) from each other (Fig. 6). For coral DOM, there was also a significant effect of treatment (ANOVA: $F_{3,28} = 14.439$, $p < 0.0001$) with the SS and DS treatment groups consuming significantly more coral DOM (Tukey's HSD, $p > 0.05$) compared to DD and SD, which were not significantly different from each other (Fig. 6). For live POM (i.e., plankton), there was a significant effect of treatment (ANOVA: $F_{3,28} = 14.094$,

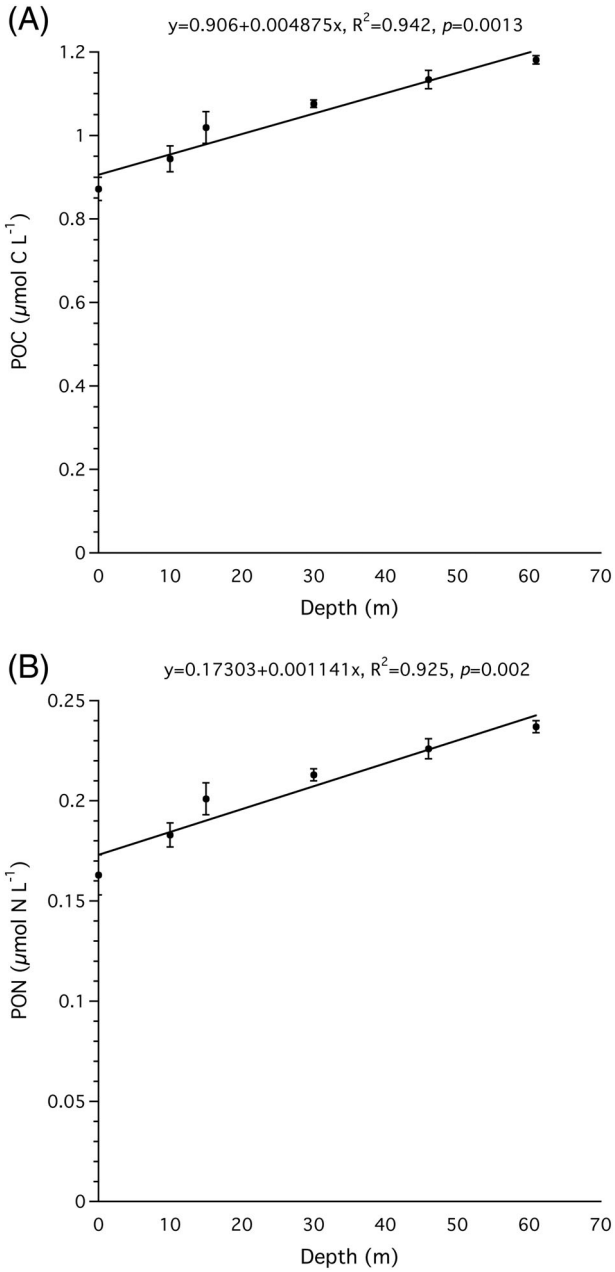

Fig. 3. Significant depth-dependent regressions for (**A**) POC (ANOVA: $F_{1,5} = 64.89$, $p = 0.0013$) and (**B**) PON (ANOVA: $F_{1,5} = 49.05$, $p = 0.002$) as a function of depth.

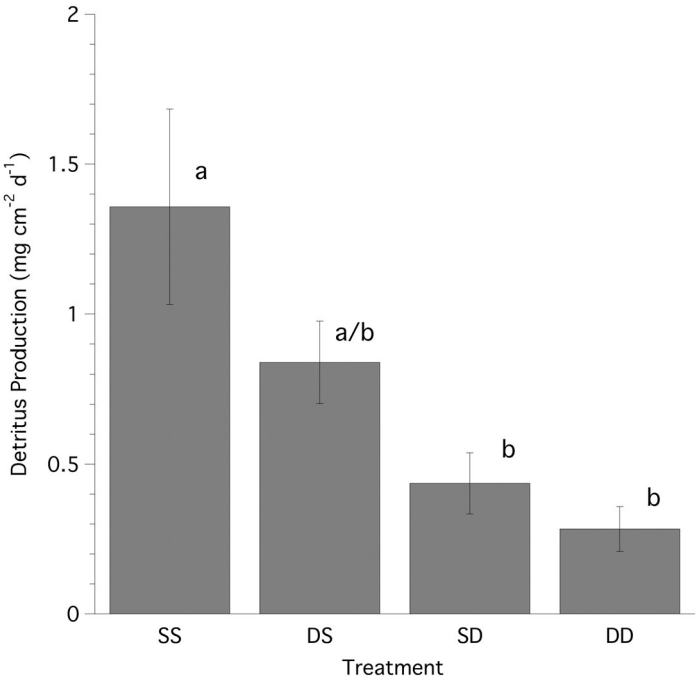

Fig. 4. Rates of detritus production for *H. caerulea* during transplant experiments. Significant treatment effects were detected (ANOVA: $F_{3,20}$ = 6.54, p = 0.0029). Treatment groups with similar superscripts are not significantly different (p < 0.05) than from each other based on *post-hoc* analysis using Tukey's HSD.

p < 0.0001) with the SS and DS treatment groups consuming significantly less POM (Tukey's HSD, p > 0.05) compared to DD and SD, which were not significantly different from

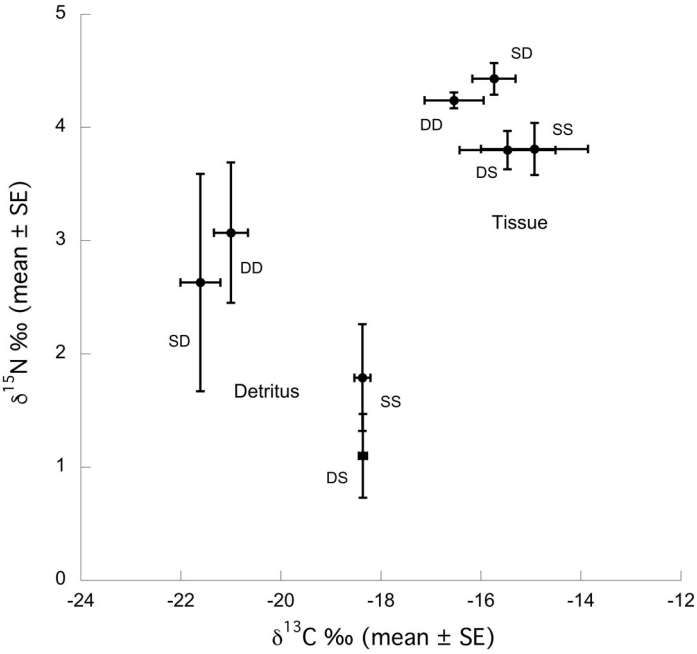

Fig. 5. Bivariate plot of δ^{13}C and δ^{15}N for bulk stable isotopic signatures (mean ± SE) of tissue and detritus samples from transplant experiment of *H. caerulea*.

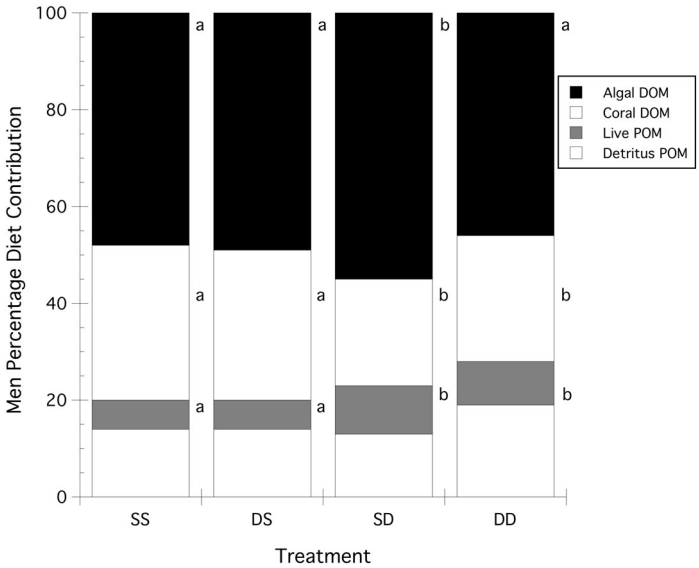

Fig. 6. Stable isotope mixing model results for *H. caerulea*. Percentage of source endmembers for algal and coral DOM, POM, and detritus. Food sources with common superscript are not significantly different from each other (Tukey's HSD > 0.05).

each other (Fig. 6). Lastly, there was no significant effect of treatment on the percentage of detrital POM contributing to the diet of experimental sponges (ANOVA: $F_{3,28}$ = 2.043, p = 0.0131) (Fig. 6).

Microbial composition and function of sponge microbiomes

For the microbiome community, a multidimensional analysis of the Beta diversity estimates using Bray–Curtis distance matrices at the class level (Fig. 7A) for the treatment, ambient seawater and detritus samples showed a significant effect of treatment (PERMANOVA: $F_{3,24}$ = 1.98, p = 0.002). All treatment samples were significantly different in their microbial composition from their surrounding seawater and detritus, and seawater and detritus were significantly different from each other (Fig. 7A). Post hoc PERMANOVA on the different treatment groups revealed significant differences between the SD and DD treatments (PERMANOVA: $F_{1,12}$ = 2.38, Bonferroni-corrected p = 0.02), the SD and DS treatments (PERMANOVA: $F_{3,24}$ = 1.98, Bonferroni-corrected p = 0.024), and the SS and DD treatments (PERMANOVA: $F_{3,24}$ = 1.98, Bonferroni-corrected p = 0.018). The composition of the *H. caerulea* tissue consisted of 54 class level assignments among all treatment groups. Working with those classes that consisted of greater than 1% of the relative abundance (13 classes; Fig. 7B), significant differences were found at the class level (Table **S1**), where significant post hoc comparisons occurred for the SS vs. DD treatments for the *Oxyphotobacteria*, which included the genera *Cyanobium*, *Prochlorococcus*, and *Synechococcus*, where the SS treatment had a significantly greater abundance (Tukey's HSD, p < 0.05; Table **S1**

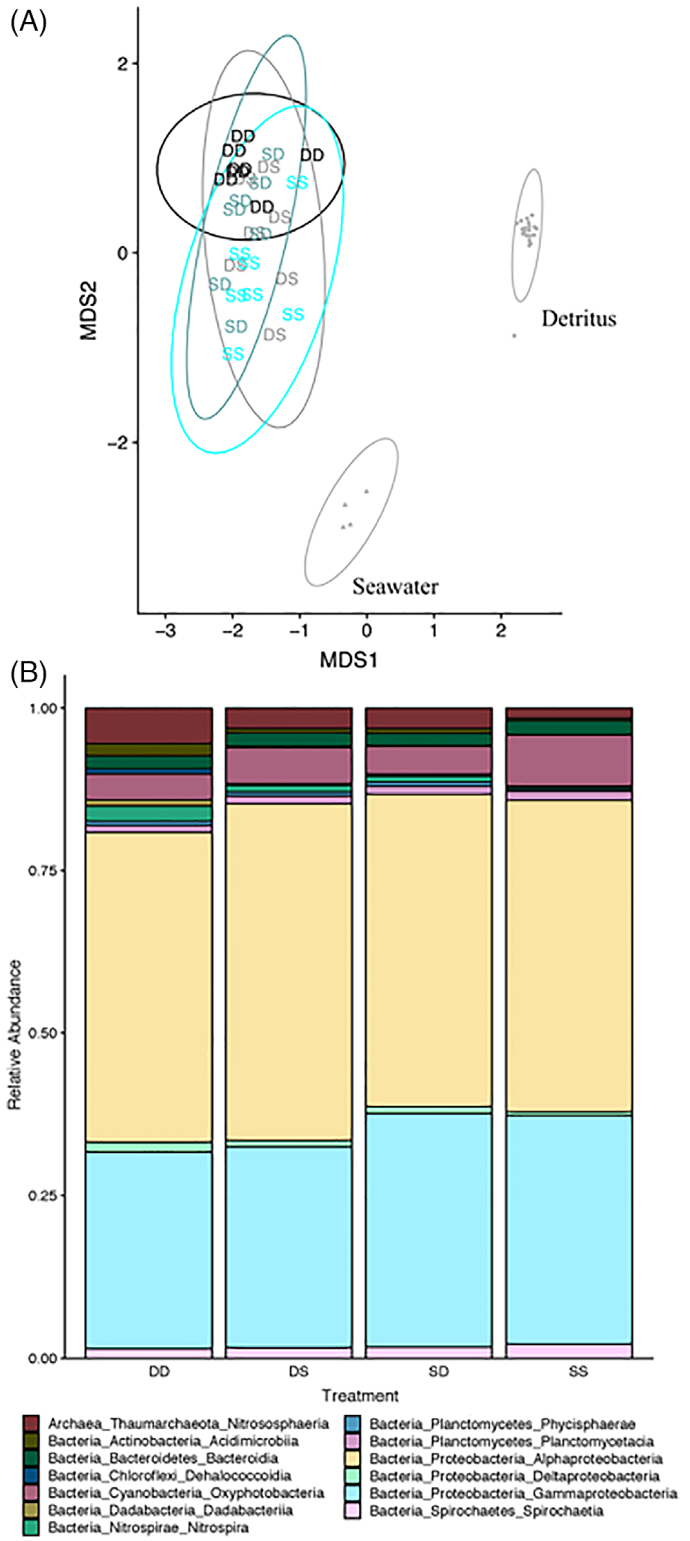

Fig. 7. (**A**) Multidimensional analysis of the β-diversity estimates using Bray–Curtis distance matrices at the class level for the experimental treatments, ambient seawater and detritus samples. 95% confidence interval (CI) ellipses are drawn to denote common treatment groups. (**B**) Average relative abundance of OTUs (97% similarity) at the class level for each treatment group for *H. caerulea* samples from the transplant experiment.

and Fig. 7B). For the DD samples *Acidimicrobiia*, *Nitrososphaeria*, *Nitrospira*, *Deltaproteobacteria*, and *Dadabacteriia* were significantly higher (Tukey's HSD, $p < 0.05$; Table **S1**) in abundance (Fig. 7B). In addition, for *Acidomicrobiia* and *Nitrospira*, the DS vs. DD and SD vs. DD pairwise comparisons were also significantly different (Tukey's HSD, $p < 0.05$; Table **S1**).

For *H. caerulea*, those genes involved in carbon metabolism (KEGG pathway 01200) showed no significant effects when all treatments were considered. Subsequently, the analysis was collapsed to analyze only shallow (SS and DS) vs. deep (DD and SD) samples. Genes for carbon fixation (ribulose-1,5-bisphosphate carboxylase/oxygenase [RuBisco]), small chain, KO1602) were significantly enriched (ANOVA: $F_{1,26}$ = 12.8, FDR corrected p = 0.014) in shallow vs. deep samples, whereas chitin degradation (chitin disaccharide deacetylase, K03478) was significantly enriched (ANOVA: $F_{1,26}$ = 18.6, FDR corrected p = 0.019) in deep vs. shallow samples. No genes for nitrogen metabolism (KEGG pathway 00910) were significantly different between shallow and deep samples.

Discussion

Most of the available substrate on a coral reef is found in the three-dimensional framework of its cryptic spaces and marine caves, estimated to be 75–90% of total reef volume (Ginsburg 1983), and dominated by sponges (e.g., Jackson and Winston 1982; Richter et al. 2001; van Duyl et al. 2006; Slattery et al. 2013). It has been shown that the majority of organic carbon removal by the reef framework, > 95% for both Indo-Pacific and Caribbean regions, is in the form of DOC (de Goeij and van Duyl 2007). Many of the sponges commonly found in, but not restricted to, cryptic environments, including *H. caerulea*, have been shown to utilize DOC (de Goeij et al. 2008*a*), and they release a significant amount of carbon as detritus (de Goeij et al. 2013; Alexander et al. 2014; Rix et al. 2016, 2017). This led to the formulation of the sponge-loop hypothesis, where DOM taken up by sponges is subsequently released as detritus, which then enters the benthic detrital food chain (de Goeij et al. 2013). While the ubiquity of the sponge loop is gaining support in different tropical (i.e., Red Sea) and even deep-sea coral reef habitats (Rix et al. 2016, 2018), some of the early uncertainties, such as the influence of depth and food availability on sponge-loop fluxes, and the difference between cryptic and open reef sponges in detritus production (Slattery and Lesser 2015; Pawlik et al. 2015*a*,*b*), remain unanswered. Here, we have shown that for *H. caerulea*, the rate of detritus production at mesophotic depths (i.e., 50 m) was significantly lower than conspecifics at shallow depths (i.e., 10 m). This is significant because it suggests that populations of *H. caerulea* at mesophotic depths may: (1) exhibit depth-specific differences in the microbiome that may influence detritus production due to differences in DOM composition, bioavailability, and utilization (e.g., coral vs. algal-derived DOM) and/or (2) shift energy from cell turnover (= maintenance costs) to increased net biomass

(= costs of growth) which includes new choanocyte chambers, and potentially less detritus production, because of better quality food (i.e., greater assimilation efficiencies of more abundant, low C : N, POM vs. DOM), especially when combined with increased clearance rates at mesophotic depths.

Detritus production occurs whether POM or DOM is consumed (Maldonado 2015), and tracer studies have shown that algal-derived DOM is incorporated at a higher rate by the microbiome whereas the incorporation of coral-derived DOM occurs at a higher rate by the sponge host (Rix et al. 2017). For the samples in this experiment, the sponge tissue and sponge-derived detritus samples were completely separated from each other based on their bulk stable isotopic values (Fig. 5). Compared to previous work on *H. caerulea* from the same location, the δ^{15}N tissue values are similar (van Duyl et al. 2011), while the δ^{13}C stable isotope values for sponge tissues from this study are enriched in ^{13}C by $\sim$ 2.5 relative to DOM suggesting the broad use of DOM as a food source (de Goeij et al. 2008*b*), and macroalgal-derived DOM in particular. Additionally, van Duyl et al. (2011) used the same mixing model and estimated that 74.8% of the diet of *H. caerulea* originates from coral-derived mucus in shallow, cryptic environments, from which up to 80% enters the DOM pool (Wild et al. 2004). However, van Duyl et al. (2011) did not include macroalgal-derived DOM sensu stricto (i.e., crustose coralline algae were used as a proxy) in their analysis, which may contribute a significant amount of the available DOM on open coral reefs, and sponges have been shown to utilize it as a food source (van Duyl et al. 2018). The δ^{13}C stable isotope values of sponge-derived detritus signatures, however, were enriched in ^{13}C by $\sim$ 2.0–4.0‰ relative to POM suggesting that the isotopic value of sponge-derived detritus is influenced by the consumption of POM.

Using these SIA values, the isotope mixing model results for *H. caerulea* show that all sponges in these experiments use $\sim$ 1.5–2.0 times as much algal-derived DOM relative to coral-derived DOM suggesting that the microbiome may have had a greater impact on the assimilation of DOM (Rix et al. 2017). However, while it has been shown that detritus production for algal-derived DOM occurs at higher rates than for coral-derived DOM (Rix et al. 2017), rates of detritus production for mesophotic *H. caerulea* are lower despite a DOM resource primarily from macroalgae, and cyanobacterial mats (Brocke et al. 2015; de Bakker et al. 2017). This could imply that the overall lower concentration of DOM at mesophotic depths caused the decrease in detritus production, or alternatively, shallow-water sponges acquire more algal-derived DOM from internal sources such as the translocation of DOM from the photosynthetic cyanobacteria in their microbiome. While the irradiances that these sponges were exposed to are equivalent such that rates of cyanobacterial productivity might not differ, the cyanobacteria in the microbiome of *H. caerulea* are distinct from the water column (Shannon–Weaver alpha-diversity index, PERMANOVA: $F_{1,30}$ = 7.56, p = 0.001), with sponge cyanobacteria comprised of seven genera while seawater from both 10 and 50 m is dominated by two genera (Fig. S2), and are present in greater abundances in SS vs. DD treatments. Taken together, the bulk δ^{13}C values of *H. caerulea* tissues and detritus represents a mixed diet of both DOM (derived from macroalgae and coral) and POM, and based on the mixing model of the relative consumption of different trophic resources, POM consumption increases with increasing depth consistent with its increased availability as depth increases (Lesser 2006; Lesser and Slattery 2013; Slattery and Lesser 2015).

Mesophotic sponges have increased amounts of POM available and decreased amounts of DOM compared with their shallow-water counterparts (Figs. 1, 2), but what role would the modest amounts of increased POM have in detritus production for these sponges? The isotopic signatures of the detritus produced by these sponges shows lower δ^{13}C and δ^{15}N values which likely represent both sponge-derived detritus, as well as water column detrital POM not produced by sponges, given that these sources of detritus could not be separated in these analyses (i.e., controls were subtracted for calculating rates of detritus production but could not be subtracted for other analyses). The colonization of the detrital POM and sponge-derived detritus by bacteria, both bacterioplankton and bacteria from the microbiome, and eukaryote detritivores from the surrounding seawater and from sponge-associated detritivores is also likely to have occurred. The C : N ratios of sponge-derived detritus (8.46 $\pm$ 0.33 [SE]) across all treatments were significantly (two-tailed t-test, $t(58)$ = 7.62, $p < 0.0001$) higher than the sponge tissues (5.48 $\pm$ 0.23 [SE]), which is consistent with detritus produced during laboratory studies (Rix et al. 2016). This is not that surprising given the presence, albeit in low concentrations for an LMA sponge, of low C : N bacteria in the microbiome and their potential influence on the C : N ratio of the sponge holobiont. However, the confounding signals from these bacteria, detritovores and bacterivores colonizing the detritus make interpreting the detritus isotopic values, relative to the sponge tissue, difficult at best.

Based on the total organic carbon (i.e., both POC and DOC) available to sponges at shallow and mesophotic depths, the sponges used in this study do not appear to be limited by the availability of carbon. In addition, the C : N ratios of sponge tissues from both shallow and mesophotic depths, ranging from 5.2 to 6.2, strongly suggest carbon sufficiency. A number of studies, however, have suggested that sponges may be limited by the availability of nitrogen (Hadas et al. 2009; Rix et al. 2016; de Goeij et al. 2017; Lesser et al. 2018). This is because DOM in the open, oligotrophic waters of coral reefs has a high C : N ratio (> 10: Ogawa and Tanoue 2003; Tanaka et al. 2011; Rix et al. 2016), such that one would hypothesize that if sponges depend on DOM for a large proportion of their carbon this would result in nitrogen limitation and the need for other sources of nitrogen such as POM (Hadas et al. 2009), or potentially through internal recycling of nitrogen between the sponge and it is microbiome (Hoffmann et al. 2009). In this study, the concentration of DOM at mesophotic depths was

lower than shallow depths, but the C : N ratio of mesophotic DOM (~ 21) was greater than that of shallow DOM (~ 14), initially suggesting a depletion of N with depth. However, only ~ 20% of DOC is bioavailable in shallow reef waters (de Goeij and van Duyl 2007; Lønborg and Álvarez-Salgado 2012; Lønborg et al. 2017) and potentially even lower at mesophotic depths. If we assume 10% bioavailability for the deeper depths, and we also assume the bioavailability of DON tracks DOC, then the C : N ratios for shallow (~ 14) and mesophotic (~ 21) DOM are still sufficient to support metabolism in terms of the availability of carbon. But if 40–70% or more of DOC uptake is used to fulfill respiratory requirements in *H. caerulea* (de Goeig et al. 2008*a*; Hadas et al. 2009; Morganti et al. 2017; Hoer et al. 2018), then the remaining carbon, along with the available nitrogen, should also be sufficient to support balanced growth as it results in a lower mean C : N for DOM of ~ 8.64 and 4.32 for shallow sponges at 40% and 70% of carbon respired and ~ 6.35 and 3.18 for upper mesophotic sponges (Table S3). In addition, the live POM C : N ratios are low, and do not differ significantly across the shallow to mesophotic depth gradient (~ 5). As a result, we have no reason to suspect any carbon or nitrogen limitation from shallow to mesophotic depths relative to growth in *H. caerulea*. Our calculations suggest that had this been one of the ~ 50% of LMA sponges that do not utilize DOM (de Goeij et al. 2017; Morganti et al. 2017), the DOM available to sponges, after satisfying standard metabolic requirements (i.e., 70% of DOC is respired), would have been significantly nitrogen limited in shallow waters (C : N ~ 30.55) compared to mesophotic depths (C : N ~ 14.12). As a result, the POM fraction, while small, is an increasingly important source of nitrogen to offset decreases in DON with increasing depth for growth of the sponge host, as the sponge microbiome is not likely to ever be nitrogen limited due to the abundant *in hospite* concentrations of DIN.

Most sponges have been found to consume food, both POM and DOM, in amounts proportional to the abundance of these resources (Pile 1997; Lesser 2006; de Goeij et al. 2008*a*). Despite suggestions to the contrary that sponges are actively selecting different food resources (McMurray et al. 2016), most sponges appear to passively select particles based on the functional morphology of their feeding apparatus and the size-selective constraints imposed by the choanocytes (Hadas et al. 2009; Maldonado et al. 2012). If DOM, as described above, is sufficient to support the energetic and biosynthetic requirements for maintenance metabolism, then the additional low C : N POM can be used for sponge host growth, especially if consumed in proportion to its availability. Sponges increase in percent cover and abundance with increasing depth (Lesser and Slattery 2018), as DOM resources decrease with depth and POM resources increase. This observation has led to suggestions that sponges may be nitrogen limited in regards to the total sponge biomass that can be supported (de Goeij et al. 2017; Lesser et al. 2018). But in this study, the C : N ratio of both DOM and POM (see above) does not support either qualitative, or quantitative, carbon or nitrogen limitation across the shallow to mesophotic gradient. Given this, the primary restriction to increased sponge growth and biomass accumulation at increasing depths would be the amount of DOM and POM consumed to support the growth, biomass, and greater abundance of sponges from shallow to mesophotic depths (Ribes et al. 2003, 2005; Lesser 2006; Lesser and Slattery 2018). Consuming a more stoichiometrically balanced (i.e., lower C : N) diet across the shallow to mesophotic depth gradient is essential, but in order to support the faster growth and greater biomass of mesophotic sponges consuming more food with increasing depth appears to be required. Given that a proportional increase in the uptake of DOM and POM occurs as resources increase (e.g., Morganti et al. 2017), the rate of sponge pumping would also be important. Rates of sponge pumping (i.e., Q values) do increase with increasing depth, at least down to 30 m (Fig. S3), and if true into the mesophotic zone more food would be consumed with increasing depth. When food is qualitatively, or quantitatively, limiting most marine invertebrates conserve maintenance metabolism at the expense of growth, and when food is not limiting, then both higher rates of growth and biomass accumulation can be supported (Fraser and Roger 2007; Sololova et al. 2012). The efficient assimilation of low C : N resources into energetically more expensive biomass production vs. maintenance (= cell turnover and detritus production) might subsequently decrease the amount of detritus produced as depth increases.

Sponges contain diverse microbial communities within their tissues (Hentschel et al. 2002, 2012; Taylor et al. 2007) that are, in part, known to be responsible for the ability of sponges to uptake and process DOM (de Goeij et al. 2008*b*; Rix et al. 2016, 2017). Additionally, sponge microbiomes can be structured by environmental factors such as light or nutrients that vary with depth (e.g., Morrow et al. 2016). The microbiome communities of *H. caerulea* are structured by their native depths, the effect of which is not significantly diminished by short-term experimental transplantation. However, while transplant treatments (i.e., SD and DS) do not differ from either SS or DD treatments, they do differ from each other suggesting that microbial composition has begun transitioning toward communities more characteristic of the transplanted depth over a period of 10 d. The microbiome of *H. caerulea* is dominated by 13 classes of prokaryotes (Fig. 5B) for which significant treatment effects were only observed for the *Oxyphotobacteria*, *Nitrososphaeria*, *Acidimicrobiia*, *Nitrospira*, *Dadabacteriia*, and *Deltaproteobacteria* (Table **S1**). Members of the *Oxyphotobacteria* (= *Cyanobacteria*) are found in significantly greater abundances in shallow treatments. Photosynthetic cyanobacteria have been reported to be the most abundant group within the microbiome of many sponge species (Steindler et al. 2005; Usher, 2008; Thacker and Freeman 2012), and in previous studies the transfer of carbon rich organic material (e.g., glycerol) from cyanobacterial

symbionts to their sponge hosts has been shown (Wilkinson 1979). Since the productivity potential of cyanobacteria is related to light levels, which are equivalent between the shallow and mesophotic treatments, it is reasonable to assume that shallow populations of *H. caerulea* are receiving more translocated DOM from their symbionts as a result of their greater abundance in the shallow treatments, as well as what they uptake from their environment, and where they also produce more detritus. However, *Nitrososphaeria*, *Acidimicrobiia*, *Nitrospira*, *Dadabacteriia*, and *Deltaproteobacteria* were all significantly more abundant in DD treatments. These taxa are involved in ammonia oxidation, organic matter decomposition, heterotrophy/autotrophy/nitrite oxidation, heterotrophy/nitrite reduction, and sulfate/sulfur reduction, respectively. These metabolic capabilities include many steps in the mineralization of organic material, as well as both the nitrogen and sulfur cycles. While a linkage between differences in metabolic capabilities have been suggested for HMA vs. LMA sponges (Weisz et al. 2008), similar differences along environmental gradients, such as shifts in the abundance of specific groups within a common microbiome, have not yet been fully explored. Here, the differential abundance of specific microbial taxa in the host microbiome with changing depth predicts that these sponges can alter their metabolic phenotype to either increased primary productivity (e.g., increased abundance of RuBisco genes in shallow sponge microbiome) or enhanced metabolic capabilities to process organic material (e.g., increased abundance of genes to degrade chitin in mesophotic sponge populations).

We have shown that the sponge *H. caerulea* produces significantly less detritus at mesophotic depths than conspecifics at shallow depths, and that transplanting these populations initiates immediate changes in detritus production, trophic ecology, and shifts in their microbiome in response to their environment and availability of trophic resources. Sponges increase in abundance with increasing depth into the lower mesophotic (> 60 m) zone (Lesser and Slattery 2018). Simultaneously, DOM continues to decrease while POC increases with increasing depth into the lower mesophotic zone (Lesser et al. 2019), making it essential to understand the differential uptake, assimilation and incorporation of DOM and POM, and the potential that increased growth efficiencies are responsible for decreases in detritus production and increased sponge biomass with increasing depth.

References

Alexander, B. E., and others. 2014. Cell turnover and detritus production in marine sponges from tropical and temperate benthic ecosystems. PLoS One **9**: e109486. doi:10.1371/journal.pone.0109486

Alexander, B. E., M. Achlatis, R. Osinga, H. G. van der Geest, J. P. Cleutjens, B. Schutte, and J. M. de Goeij. 2015. Cell kinetics during regeneration in the sponge *Halisarca caerulea*: How local is the response to tissue damage? PeerJ **3**: e820. doi:10.7717/peerj.820

Apprill, A., S. McNally, R. Parsons, and L. Weber. 2015. Minor revision to V4 region SSU rRNA 806R gene primer greatly increases detection of SAR11 bacterioplankton. Aquat. Microb. Ecol. **75**: 129–137. doi:10.3354/ame01753

Barbera, P., A. M. Kozlov, L. Czech, B. Morel, D. Darriba, T. Flouri, and A. Stamatakis. 2019. EPA-ng: Massively parallel evolutionary placement of genetic sequences. Syst. Biol. **68**: 365–369. doi:10.1093/sysbio/syy054

Bell, J. J. 2008. The functional roles of marine sponges. Estuar. Coastal Shelf. Sci. **79**: 341–353. doi:10.1016/j.ecss.2008.05.002

Bell, J. J., and others. 2018*a*. Climate change alterations to ecosystem dominance: How might sponge-dominated reefs function. Ecology **99**: 1920–1931. doi:10.1002/ecy.2446

Bell, J. J., H. M. Bennett, A. Rovellini, and N. S. Webster. 2018*b*. Sponges to be winners under near-future climate scenarios. Bioscience **68**: 955–968. doi:10.1093/biosci/biy142

Bertilsson, S., O. Berglund, D. M. Karl, and S. W. Chisholm. 2003. Elemental composition of marine *Prochlorococcus* and *Synechococcus*: Implications for the ecological stoichiometry of the sea. Limnol. Oceanogr. **48**: 1721–1731. doi:10.4319/lo.2003.48.5.1721

Brocke, H. J., F. Wenzhoefer, D. de Beer, B. Mueller, F. C. van Duyl, and M. M. Nugues. 2015. High dissolved organic carbon release by benthic cyanobacterial mats in a Caribbean reef ecosystem. Sci. Rep. **5**: 8852. doi:10.1038/srep08852

Callahan, B. J., P. J. McMurdie, M. J. Rosen, A. W. Han, A. J. A. Johnson, and S. P. Holmes. 2016. DADA2: High-resolution sample inference from Illumina amplicon data. Nat. Methods **13**: 581–583. doi:10.1038/nmeth.3869

Campbell, L., H. A. Nolla, and D. Vaulot. 1994. The importance of *Prochlorococcus* to community structure in the central North Pacific Ocean. Limnol. Oceanogr. **39**: 954–960. doi:10.4319/lo.1994.39.4.0954

de Bakker, D. M., F. C. van Duyl, R. P. M. Bak, M. N. Nugues, G. Nieuwland, and E. H. Meesters. 2017. 40 years of benthic community change on the Caribbean reefs of Curaçao and Bonaire: The rise of slimy cyanobacterial mats. Coral Reefs **36**: 355–367. doi:10.1007/s00338-016-1534-9

de Goeij, J. M., and F. C. van Duyl. 2007. Coral cavities are sinks of dissolved organic carbon (DOC). Limnol. Oceanogr. **52**: 2608–2617. doi:10.4319/lo.2007.52.6.2608

de Goeij, J. M., H. van den Berg, M. M. van Oostveen, E. H. G. Epping, and F. C. van Duyl. 2008*a*. Major bulk dissolved organic carbon (DOC) removal by encrusting coral reef cavity sponges. Mar. Ecol. Prog. Ser. **357**: 139–151. doi:10.3354/meps07403

de Goeij, J. M., L. Moodley, M. Houtekamer, N. M. Carballeira, and F. C. van Duyl. 2008*b*. Tracing C^{13}-enriched dissolved and particulate organic carbon in the bacteria-containing coral reef sponge *Halisarca caerulea*: Evidence for DOM feeding. Limnol. Oceanogr. **53**: 1376–1386. doi:10.4319/lo.2008.53.4.1376

de Goeij, J. M., D. van Oevelen, M. J. A. Vermeij, R. Osinga, J. J. Middelburg, A. F. P. M. de Goeij, and W. Admiral. 2013. Surviving in a marine desert: The sponge loop retains resources within coral reefs. Science **342**: 108–110. doi:10.1126/science.1241981

de Goeij, J. M., M. P. Lesser, and J. R. Pawlik. 2017. Nutrient fluxes and ecological functions of coral reef sponges in a changing ocean, p. 373–564. *In* J. L. Carballo and J. J. Bell [eds.], Climate change, ocean acidification and sponges. Springer International. doi:10.1007/978-3-319-59008-0_8

Ducklow, H. W., D. L. Kirchman, H. L. Quinby, C. A. Carlson, and H. G. Dam. 1993. Stocks and dynamics of bacterioplankton carbon during the spring bloom in the eastern North Atlantic Ocean. Deep-Sea Res. **40**: 245–263. doi:10.1016/0967-0645(93)90016-G

Diaz, M. C., and K. Rützler. 2001. Sponges: An essential component of Caribbean coral reefs. Bull. Mar. Sci. **69**: 535–546.

Eddy, S. R. 2008. A probabilistic model of local sequence alignment that simplifies statistical significance estimation. PLoS Comput. Biol. **4**: e1000069. doi:10.1371/journal.pcbi.1000069

FaggerBakke, K. M., M. Heldal, and S. Norland. 1996. Content of carbon, nitrogen, oxygen, sulfur and phosphorus in native aquatic and cultured bacteria. Aquat. Microb. Ecol. **10**: 15–27. doi:10.3354/ame010015

Fiore, C., J. K. Jarett, N. D. Olson, and M. P. Lesser. 2010. Nitrogen fixation and nitrogen transformations in marine symbioses. Trends Microbiol. **18**: 455–463. doi:10.1016/j.tim.2010.07.001

Fiore, C. L., D. M. Baker, and M. P. Lesser. 2013*a*. Nitrogen biogeochemistry in the Caribbean sponge *Xestospongia muta*: A source or sink of dissolved inorganic nitrogen? PLoS One **8**: e72961. doi:10.1371/journal.pone.0072961

Fiore, C. L., J. K. Jarett, and M. P. Lesser. 2013*b*. Symbiotic prokaryotic communities from different populations of the giant barrel sponge, *Xestospongia muta*. Microbiolopen **2**: 938–952. doi:10.1002/mbo3.135

Fraser, K. P. P., and A. D. Rogers. 2007. Protein metabolism in marine animals: The underlying mechanism of growth. Ad. Mar. Biol. **52**: 267–362. doi:10.1016/S0065-2881(06)52003-6

Ginsburg, R. N. 1983. Geological and biological roles of cavities in coral reefs, p. 148–153. *In* D. Barnes [ed.], Perspectives on coral reefs. Townsville: Australian Institute of Marine Science.

Gloor, G. B., J. M. Macklaim, V. Pawlowsky-Glahn, and J. J. Egozcue. 2017. Microbiome datasets are compositional: And this is not optional. Front. Microbiol. **8**: 2224. doi:10.3389/fmicb.2017.02224

Haas, A. F., F. Rohwer, C. Carlson, C. Nelson, L. Wegley, J. Leichter, and J. E. Smith. 2011. Effects of coral reef benthic primary producers on dissolved organic carbon and microbial activity. PLoS One **6**: e27973. doi:10.1371/journal.pone.00227973

Hadas, E., M. Shpigel, and M. Ilan. 2009. Particulate organic matter as a food source for a coral reef sponge. J. Exp. Biol. **212**: 3643–3650. doi:10.1242/jeb.027953

Hentschel, U., J. Hopke, M. Horn, A. B. Friedrich, M. Wagner, J. Hacker, and B. S. Moore. 2002. Molecular evidence for a uniform microbial community in sponges from different oceans. Appl. Environ. Microbiol. **68**: 4431–4440. doi:10.1128/AEM.68.9.4431-4440.2002

Hentschel, U., J. Piel, S. M. Degnan, and M. W. Taylor. 2012. Genomic insights into the marine sponge microbiome. Nat. Rev. Microbiol. **10**: 641–675. doi:10.1038/nmicro2839

Hoer, D. R., P. J. Gibson, J. P. Tommerdahl, N. L. Lindquist, and C. S. Martens. 2018. Consumption of dissolved organic carbon by Caribbean reef sponges. Limnol. Oceanogr. **63**: 337–351. doi:10.1002/lno.10634

Hoffmann, F., and others. 2009. Complex nitrogen cycling in the sponge *Geodia barretti*. Env. Microbiol. **11**: 2228–2243. doi:10.1111/j.1462-2920.2009.01944.x

Jackson, J. B. C., and J. E. Winston. 1982. Ecology of cryptic coral reef communities. I. Distribution and abundance of major groups of encrusting organisms. J. Exp. Mar. Biol. Ecol. **57**: 135–147. doi:10.1016/0022-0981(82)90188-5

Jaschinski, S., T. Hansen, and U. Sommer. 2008. Effects of acidification in multiple stable isotope analyses. Limnol Oceanogr.: Methods **6**: 12–15. doi:10.4319/lom.2008.6.12

Lahti, L., and others. 2017. Tools for microbiome analysis in R. Microbiome package version 1.5.28. Available from http://microbiome.github.com/microbiome

Lesser, M. P., S. E. Shumway, S. E, T. Cucci, and J. Smith. 1992. Impact of fouling organisms on mussel rope culture: Interspecific competition for food among suspension-feeding invertebrates. J. Exp. Mar. Biol. Ecol. **165**: 91–102. doi:10.1016/0022-0981(92)90291-H

Lesser, M. P. 2006. Benthic-pelagic coupling on coral reefs: Feeding and growth of Caribbean sponges. J. Exp. Mar. Biol. Ecol. **328**: 277–288. doi:10.1016//j.jembe.2005.07.010

Lesser, M. P., and M. Slattery. 2013. Ecology of Caribbean sponges: Are to-down or bottom-up processes more important? PloS One **8**: e79799. doi:10.1371/journal.pone.0079799

Lesser, M. P., M. Slattery, and C. D. Mobley. 2018. Biodiversity and functional ecology of mesophotic coral reefs. Ann. Rev. Ecol. Syst. **49**: 49–71. doi:10.1146/annrev-ecolsys-110617-062423

Lesser, M. P., and M. Slattery. 2018. Sponge density increases with depth throughout the Caribbean. Ecosphere **9**: e02525. doi:10.1002/ecs2.2525

Lesser, M. P., M. Slattery, J. H. Laverick, K. J. Macartney, and T. Bridge. 2019. Global community breaks at 60 m on mesophotic coral reefs. Glob. Ecol. Biogeogr. **28**: 1403–1416. doi:10.1111/geb.12940

Lønborg, C., and X. A. Álvarez-Salgado. 2012. Recycling versus export of bioavailable dissolved organic matter in the coastal ocean and efficiency of the continental shelf pump. Global Biogeochem. Cycles **26**: GB3018. doi:10.1029/2012GB004353

Lønborg, C., X. A. Álvarez-Salgado, S. Duggan, and C. Carreira. 2017. Organic matter bioavailability in tropical coastal waters: The great barrier reef. Limnol. Oceanogr. **63**: 1015–1035. doi:10.1002/lno.10717

Louca, S., and M. Doebeli. 2018. Efficient comparative phylogenetics on large trees. Bioinformatics **34**: 1053–1055. doi:10.1093/bioinformatics/btx701

Louchard, E. M., P. R. Reid, C. F. Stephens, C. O. Davis, R. A. Leathers, and T. V. Downes. 2003. Remote sensing of benthic habitats and bathymetry in coastal environments at Lee Stocking Island, Bahamas: A comparative spectral classification approach. Limonol. Oceanogr. **48**: 511–521. doi:10.4319/lo.2003.48.1_part_2.0511

Maldonado, M. 2015. Sponge waste that fuels marine oligotrophic food webs: A re-assessment of its origin and nature. Mar. Ecol. **37**: 477–491. doi:10.1111/maec.12256

Maldonado, M., M. Ribes, and F. C. van Duyl. 2012. Nutrient fluxes through sponges: biology, budgets, and ecological implications. Adv. Mar. Biol. **62**: 113–182. doi:10.1016/B978-0-12-394283-8.00003-5

McMurray, S. E., Z. I. Johnson, D. E. Hunt, J. R. Pawlik, and C. M. Finelli. 2016. Selective feeding by the giant barrel sponge enhances foraging efficiency. Limnol. Oceanogr. **61**: 1271–1286. doi:10.1002/lno.10287

McMurray, S. E., A. D. Subler, P. M. Erwin, C. M. Finelli, and J. R. Palik. 2018. A test of the sponge-loop hypothesis for emergent Caribbean reef sponges. Mar. Ecol. Prog. Ser. **588**: 1–14. doi:10.3354/meps12466

McMurdie, P. J., and S. Holmes. 2013. Phyloseq: An R package for reproducible interactive analysis and graphics of microbiome census data. PLoS One **8**: e61217. doi:10.1371/journal.pone.0061217

Morel, A., Y. H. Ahn, F. Partensky, D. Vaulot, and H. Claustre. 1993. *Prochlorococcus* and *Synechococcus*: A comparative study of their optical properties in relation to their size and pigmentation. J. Mar. Res. **51**: 617–649. doi:10.1357/0022240933223963

Morganti, T., R. Coma, G. Yahel, and M. Ribes. 2017. Trophic niche separation that facilitates co-existence of high and low microbial abundance sponges is revealed by in situ study of carbon and nitrogen fluxes. Limnol. Oceangr. **62**: 1963–1983. doi:10.1002/lno.10546

Morrow, K. M., C. L. Fiore, and M. P. Lesser. 2016. Environmental drivers of microbial community shifts in the giant barrel sponge, *Xestospongia muta*, over a shallow to mesophotic depth gradient. Environ. Microbiol. **18**: 2025–2038. doi:10.1111/1462-2920.13226

Mueller, B., J. M. de Goeij, M. J. A. Vermeij, Y. Mulders, E. van der Ent, M. Ribes, and F. C. van Duyl. 2014*a*. Natural diet of coral-excavating sponges consists mainly of dissolved organic carbon (DOC). PLoS One **9**: e90152. doi:10.1371/journal.pone.0090152

Mueller, B., R. M. van der Zande, P. J. M. van Leent, E. H. Meesters, M. J. A. Vermeij, and F. C. van Duyl. 2014*b*. Effect of light availability on dissolved organic carbon release by Caribbean reef algae and corals. Bull. Mar. Sci. **90**: 875–893. doi:10.5343/bms.2013.1062

Mueller, B., J. Den Haan, P. M. Visser, M. J. A. Vermeij, and F. C. van Duyl. 2016. Effect of light and nutrient availability on the release of dissolved organic carbon (DOC) by Caribbean turf algae. Sci. Rep. **6**: 23248. doi:10.1038/srep23248

Mueller, B., E. H. Meesters, and F. C. van Duyl. 2017. DOC concentrations across a depth-dependent light gradient on a Caribbean coral reef. PeerJ **6**: e3456. doi:10.7717/peerj.3456

Ogawa, H., and E. Tanoue. 2003. Dissolved organic matter in oceanic waters. J. Oceanogr. **59**: 129–147. doi:10.1023/A:1025528919771

Oksanen, J., and others. 2019. vegan: Community Ecology Package. R package version 2.5-4. Available from https://CRAN.R-project.org/package=vegan

Parada, A. E., D. M. Needham, and J. A. Fuhrman. 2016. Every base matters: Assessing small subunit rRNA primers for marine microbiomes with mock communities, time series and global field samples. Environ. Microbiol. **18**: 1403–1414. doi:10.1111/1462–2920.13023

Pawlik, J. R. 2011. The chemical ecology of sponges on Caribbean reefs: Natural products shape natural systems. Bioscience **61**: 888–898. doi:10.1525/bio.2011.61.11.8

Pawlik, J. R., S. E. McMurray, P. Erwin, and S. Zvea. 2015*a*. A review of evidence for food-limitation of sponges on Caribbean reefs. Mar. Ecol. Prog. Ser. **519**: 265–283. doi:10.3354/meps11093

Pawlik, J. R., S. E. McMurray, P. Erwin, and S. Zvea. 2015*b*. No evidence for food limitation of Caribbean reef sponges: Reply to Slattery & Lesser (2015). Mar. Ecol. Prog. Ser. **527**: 281–284. doi:10.3354/meps11093

Perea-Blazquez, A., S. K. Davy, and J. J. Bell. 2012. Estimates of particulate organic carbon flowing from the pelagic environment to the benthos through sponge assemblages. PLoS One **7**: e29569. doi:10.1371/journal.pone.0029569

Pile, A. J., M. R. Patterson, and M. Savarese. 1997. Trophic effects of sponge feeding within lake Baikal's littoral zone. 2. Sponge abundance, diet, feeding efficiency, and carbon flux. Limnol. Oceanogr. **42**: 178–184. doi:10.4319/lo.1997.42.1.0178

Reiswig, H. M. 1971. Particle feeding in natural populations of three marine demosponges. Biol. Bull. **141**: 568–591. doi:10.2307/1540270

Reiswig, H. M. 1974. Water transport, respiration and energetics of three tropical sponges. J. Exp. Mar. Biol. Ecol. **14**: 231–249. doi:10.1016/0022-0981(74)90005-7

Ribes, M., R. Coma, M. J. Atkinson, and R. A. Kinzie III. 2003. Particle removal by coral reef communities: Picoplankton is a major source of nitrogen. Mar. Ecol. Prog. Ser. **257**: 13–23. doi:10.3354/meps257013

Ribes, M., R. Coma, M. J. Atkinson, and R. A. Kinzie III. 2005. Sponges and ascidians control removal of particulate organic nitrogen from coral reef water. Limnol. Oceanogr. **50**: 1480–1489. doi:10.4391/lo.2005.50.5.1480

Richter, C., M. Wunsch, M. Rasheed, I. Kötter, and M. I. Badran. 2001. Endoscopic exploration of Red Sea coral reefs reveals dense populations of cavity-dwelling sponges. Nature **413**: 726–730.

Rix, L., and others. 2016. Coral mucus fuels the sponge loop in warm- and cold-water coral reef ecosystems. Sci. Rep. **6**: 18715. doi:10.1038/srep18715

Rix, L., J. M. de Goeij, D. van Oevelen, U. Struck, F. A. Al-Horani, C. Wild, and M. S. Naumann. 2017. Differential recycling of coral and algal dissolved organic matter via the sponge loop. Funct. Ecol. **31**: 778–789. doi:10.1111/1365-2435.12758

Rix, L., J. M. de Goeij, D. van Oevelen, U. Struck, F. A. Al-Horani, C. Wild, and M. S. Naumann. 2018. Reef sponge facilitate the transfer of coral-derived organic matter to their associated fauna via the sponge loop. Mar. Ecol. Prog. Ser. **589**: 85–96. doi:10.3354/meps12443

Scheffers, S. R., R. W. van Soest, G. Nieuwland, and R. P. Bak. 2010. Coral reef framework cavities: Is functional similarity reflected in composition of the cryptic macrofaunal community? Atoll Res. Bull. **583**: 1–24. doi:10.5479/si.00775630.583.1

Seutin, G., B. N. White, and P. T. Boag. 1991. Preservation of avian blood and tissue samples for DNA analyses. Can. J. Zool. **69**: 82–90. doi:10.1139/z91-013

Slattery, M., D. J. Gochfeld, C. G. Easson, and L. R. K. O'Donahue. 2013. Facilitation of coral reef biodiversity and health by cave sponge communities. Mar. Ecol. Prog. Ser. **476**: 71–86. doi:10.3354/meps10139

Slattery, M., and M. P. Lesser. 2015. Trophic ecology of sponges from shallow to mesophotic depths (3 to 150 m): Comment on Pawlik and others. (2015). Mar. Ecol. Prog. Ser. **527**: 275–279. doi:10.3354/meps11307

Slattery, M., D. J. Gochfeld, M. C. Diaz, R. W. Thacker, and M. P. Lesser. 2016. Variability in chemical defense across a shallow to mesophotic depth gradient in the Caribbean sponge *Plakortis angulospiculatus*. Coral Reefs **35**: 11–22. doi:10.1007/s00338-015-1324-9

Sokolova, I. M., M. Frederich, R. Bagwe, G. Lannig, and A. A. Sukhotin. 2012. Energy homeostasis as an integrative tool for assessing limits of environmental tolerance in aquatic invertebrates. Mar. Environ. Res. **79**: 1–15. doi:10.1016/j.marenvres.2012.04.003

Southwell, M. W., J. B. Weisz, C. S. Martens, and N. Lindquist. 2008. In situ fluxes of dissolved inorganic nitrogen from the sponge community on conch reef, Key Largo, Florida. Limnol. Oceanogr. **53**: 986–996. doi:10.4319/lo.2008.53.3.0986

Steindler, L., D. Huchon, A. Avni, and M. Ilan. 2005. 16S rRNA phylogeny of sponge-associated cyanobacteria. Appl. Environ. Microbiol. **71**: 4127–4131. doi:10.1128/AEM.71.7.4127-4131.2005

Sunagawa, S., C. M. Woodley, and M. Medina. 2010. Threatened corals provide underexplored microbial habitats. PLoS One **5**: e9554. doi:10.1371/journal.pone.0009554

Tanaka, Y., T. Miyajima, A. Watanabe, K. Nadoaka, T. Yamamoto, and H. Ogawa. 2011. Distribution of dissolved organic carbon and nitrogen in a coral reef. Coral Reefs **30**: 533–541. doi:10.1007/s00338-011-0735-5

Taylor, M. W., R. Radax, D. Steger, and M. Wagner. 2007. Sponge-associated microorganisms: Evolution, ecology, and biotechnological potential. Microbiol. Mol. Biol. Rev. **71**: 295–347. doi:10.1128/MMBR.00040-06

Thacker, R. W., and C. J. Freeman. 2012. Sponge-microbe symbioses: Recent advances and new directions. Adv. Mar. Biol. **62**: 57–111. doi:10.1016/B978-0-12-394283-8.00002-3

Torréton, J., J. Pages, P. Dufour, and G. Cauwet. 1997. Bacterioplankton carbon growth yield and DOC turnover in some coral reef lagoons. Proc 8th Int. Coral Reef Symp. **1**: 947–952.

Usher, K. M. 2008. The ecology and phylogeny of cyanobacterial symbionts in sponges. Mar. Ecol. **29**: 178–192. doi:10.1111/j.1439-0485.2008.00245.x

van Duyl, F. C. 1985. Atlas of the living reefs of Curaçao and Bonaire (Netherlands Antilles). Utrecht. Ph.D. thesis, Vrije Universiteit.

van Duyl, F. C., S. R. Scheffers, F. I. M. Thomas, and M. Driscoll. 2006. The effect of water exchange on bacterioplankton depletion and inorganic nutrient dynamics in coral reef cavities. Coral Reefs **25**: 23–36. doi:10.1007/s00338-005-0066-5

van Duyl, F. C., L. Moodley, G. Nieuwland, L. van Ijzerloo, R. W. M. van Soest, M. Houtekamer, E. H. Meesters, and J. J. Middleburg. 2011. Coral cavity sponges depend on reef-derived food resources: Stable isotope and fatty acid constraints. Mar. Biol. **158**: 1653–1666. doi:10.1007/s00227-011-1681-z

van Duyl, F. C., B. Mueller, and E. H. Meesters. 2018. Spatio-temporal variation in stable isotope signatures ($\delta^{13}C$ and $\delta^{15}N$) of sponges on the Saba Bank. PeerJ **6**: e5460. doi:10.7717/peerj.5460

Weisz, J. B., U. Hentschel, N. Lindquist, and C. S. Martens. 2008. Linking abundance and diversity of sponge-associated microbial communities to metabolic differences in host sponges. Mar. Biol. **152**: 475–483. doi:10.1007/s00227-007-0708-y

Wild, C., M. Huettel, A. Klueter, S. G. Kremb, M. Y. M. Rasheed, and B. B. Jørgensen. 2004. Coral mucous functions as an energy carrier and particle trap in the reef ecosystem. Nature **428**: 66–70. doi:10.1038/nature02344

Wilkinson, C. R. 1979. Nutrient translocation from symbiotic cyanobacteria to coral reef sponges, p. 373–380. *In* C. Levi

and N. Boury-Esnault [eds.], Biologie des spongiaires, v. **291**. Paris, France: Colloques Internationaux du Centre National de la Recherche Scientifique.

Wulff, J. L. 2006. Resistance vs recovery: Morphological strategies of coral reef sponges. Funct. Ecol. **20**: 699–708. doi:10.1111/j.1365-2435.2006.01143.x

Yahel, G., J. H. Sharp, and D. Marie. 2003. In situ feeding and element removal in the symbiont-bearing sponge *Theonella swinhoei*: Bulk DOC is the major source for carbon. Limnol. Oceanogr. **48**: 141–149. doi:10.4319/lo.2003.48.1.0141

Ye, Y., and T. G. Doak. 2009. A parsimony approach to biological pathway reconstruction/inference for genomes and metagenomes. PLoS Comp. Biol. **5**: e1000465. doi:10.1371/journal.pcbi.1000465

Acknowledgments

This study was supported by NSF Biological Oceanography (OCE-1632348/1632333) to M.P.L. and M.S., respectively, the European Research Council (ERC) under the European Union's Horizon 2020 research and innovation program (grant agreement 715513 to J.M.G.), and by the Ecology Fund of the Royal Netherlands Academy of Arts and Sciences to B.M.

Conflict of Interest

None declared.

Submitted 05 May 2019
Revised 12 September 2019
Accepted 31 October 2019

Associate editor: James Leichter